

Estimating the bending modulus of a FtsZ bacterial-division protein filament

Eric N. Cytrynbaum*

Department of Mathematics, University of British Columbia, Vancouver, British Columbia V6T 1Z2, Canada

Yongnan Devin Li

Department of Chemistry, University of British Columbia, Vancouver, British Columbia V6T 1Z2, Canada

Jun F. Allard

Department of Mathematics, University of California, Davis, California 95616, USA

Hadi Mehrabian

Department of Chemical and Biological Engineering, University of British Columbia, Vancouver, British Columbia V6T 1Z3, Canada

(Received 21 September 2011; revised manuscript received 8 December 2011; published 3 January 2012)

FtsZ, a cytoskeletal protein homologous to tubulin, is the principle constituent of the division ring in bacterial cells. It is known to have force-generating capacity *in vitro* and has been conjectured to be the source of the constriction force *in vivo*. Several models have been proposed to explain the generation of force by the Z ring. Here we re-examine data from *in vitro* experiments in which Z rings formed and constricted inside tubular liposomes, and we carry out image analysis on previously published data with which to better estimate important model parameters that have proven difficult to measure by direct means. We introduce a membrane-energy-based model for the dynamics of multiple Z rings moving and colliding inside a tubular liposome and a fluid model for the drag of a Z ring as it moves through the tube. Using this model, we estimate an effective membrane bending modulus of 500–700 pN nm. If we assume that FtsZ force generation is driven by hydrolysis into a highly curved conformation, we estimate the FtsZ filament bending modulus to be 310–390 pN nm². If we assume instead that force is generated by the non-hydrolysis-dependent intermediate curvature conformation, we find that $B_f > 1400$ pN nm². The former value sits at the lower end of the range of previously estimated values and, if correct, may raise challenges for models that rely on filament bending to generate force.

DOI: [10.1103/PhysRevE.85.011902](https://doi.org/10.1103/PhysRevE.85.011902)

PACS number(s): 87.17.-d, 87.16.-b, 87.10.-e, 87.15.-v

I. INTRODUCTION

FtsZ is a cytoskeletal protein that plays a central role in division in nearly all of bacteria and archaea (see [1] for a recent comprehensive review). During division, FtsZ localizes to midcell and sets the division plane by forming a ring, referred to as the Z ring, about the inner surface of the cell's circumference. A homologue of tubulin, FtsZ is also a polymerizing GTPase, although it forms short single-stranded filaments [2–4] rather than microtubules. Under certain conditions, FtsZ filaments have been found to associate laterally [2,5–7], albeit weakly [8,9], a process thought to underlie Z-ring assembly. Once formed, the Z ring is thought to be the force generator that drives the cell-wall invagination machinery, although the mechanism of force generation remains unclear, as demonstrated by the diversity of recently proposed models [10–14]. A major problem in distinguishing the actual mechanism is our limited understanding of the ultrastructure of the *in vivo* Z ring, which has received some attention recently but remains unclear [15,16]. Another problem is a paucity of quantitative experimental measurements of basic physical parameters, including the bending modulus of a filament. This bending modulus is a crucial parameter that, in some of the proposed models, directly determines the scale of the force generated. In other models, this parameter must

be small, allowing the proposed force-generating mechanisms to dominate the mechanical resistance of the filaments to bending. Estimated values for the filament bending modulus range from 220 pN nm² to 56 000 pN nm². At the lower end of this range, justification comes from two studies in which the persistence length of FtsZ filaments was determined from electron microscopy (EM) images [17,18]. However, a third study measured persistence length of filaments on a mica surface using atomic force microscopy (AFM) [11]. Instead of the standard technique for measuring persistence length, they accounted for the possibility that the filaments had a nonzero preferred curvature, as suggested by several studies [19–21], and found a persistence length of 4 μ m and hence a bending modulus of 16 000 pN nm². Further justification at the higher end comes from homology with tubulin protofilaments for which a bending modulus has been estimated from microtubule stiffness and geometry to be 12 000 pN nm² [22] and by analogy with (two-stranded) actin, which has a bending modulus of 68 000 pN nm². These estimates are summarized in Table I.

To circumvent the problems associated with extracting this physical parameter from experimental systems far removed from the *in vivo* context, we take advantage of a recent set of experiments in which Z rings were reconstituted in tubular liposomes [23]. In these experiments, Osawa *et al.* mixed lipids and FtsZ proteins. The lipids formed long thin tubes with diameters roughly similar to those of rod-shaped *E. coli*, while the FtsZ accumulated into rings scattered along the length of the tube. Over time, the rings moved about, collided, and

*cytryn@math.ubc.ca

TABLE I. Estimates of the bending modulus of FtsZ polymers.

Estimation technique	Bending modulus (pN nm ²)	Source
Persistence length from EM, assuming straight	227	Huecas <i>et al.</i> [17]
Persistence length from EM, assuming straight	840	Dajkovic <i>et al.</i> [18]
From Young's modulus of tubulin	1.2×10^4	Mickey <i>et al.</i> [22]
Persistence length from EM, assuming curvature	1.6×10^4	Horger <i>et al.</i> [11]
Fitting model to liposome data	350 or >1400	This work

coalesced. As the rings thickened, invaginations appeared in the surface of the tubular liposome. This study provided direct evidence that FtsZ alone is capable of generating a membrane-constricting force. In subsequent work, by permuting the orientation of the membrane tether on the protein and the location of the protein relative to the liposome (inside and outside), the same group demonstrated that the curvature of membrane deformations correlate with the orientation of filament curvature, supporting the hypothesis that filament bending is the force generator [21,24].

Complicating this filament bending hypothesis is the multiplicity of observed curved conformations. Early *in vitro* studies suggested that guanosine triphosphate (GTP) hydrolysis induced a conformation change from straight to highly curved with a curvature of 0.08 nm^{-1} [25]. More recently, a second curved conformation has been observed with an intermediate curvature of roughly 0.01 nm^{-1} (see [1] for a detailed discussion). This intermediate conformation does not seem to require GTP hydrolysis [19,20]. There is also evidence that the straight-to-highly-curved conformation change is not strictly hydrolysis dependent. Furthermore, cell division can still proceed in a slow-hydrolyzing mutant [26], raising questions about the energy source for force generation and the place of these conformation changes in the cycling of FtsZ subunits and filaments in the Z ring.

Shlomovitz and Gov [27] proposed a comprehensive model for Z-ring formation, coalescence, and constriction-force generation that invoked membrane-mediated forces, which arise from minimization of membrane and filament mechanical energies, acting between intrinsically curved membrane-bound filaments. These forces first bring filaments together to form rings and then act between rings to draw them together, if sufficiently close, or else push them apart to a steady separation distance. Horger *et al.* [28] proposed a similar model of membrane shape in the presence of a single ring and periodically spaced rings and concluded that the ring force required to invaginate a liposome was consistent with their previous estimates from AFM studies [11].

In the present study, we use a similar modeling formalism, namely, minimization of membrane and filament mechanical energies. Rather than adopt all parameter values a priori as in those previous studies, our goal is to use the model and data to estimate parameters whose values are still uncertain and contentious. As mentioned, the FtsZ filament bending modulus is one such parameter. Using our approach to estimating it, it is necessary to also estimate the membrane bending modulus, which suffers a similar uncertainty in the modeling literature. Shlomovitz and Gov estimated the membrane bending modulus to be 40–400 pN nm while Horger *et al.*

estimated it as 10 000 pN nm. In contrast with the latter study, we do not assume anything about the number of bilayers in the liposome wall but assume only that the composite has an effective bending modulus and fit the model to data in order to estimate that modulus.

The overall structure of our approach is to couple a set of measurements from Osawa *et al.*'s published data with a set of models that can be used to estimate parameters when compared against the data. The models include (1) a filament-membrane model, similar to those of Shlomovitz and Gov [27] and Horger *et al.* [28], (2) a dynamic ring-interaction model that generalizes the one proposed by Shlomovitz and Gov [27] to allow for many rings, and (3) a computational fluid model to adapt the results of Saffman and Delbruck's classic mobility calculation [29] to the context of a ring of protein inside a cylinder. Finally, we use a Markov Chain Monte Carlo method for parameter estimation, fitting the dynamic ring-interaction model to the data obtained by tracking all rings in Osawa's time-lapse movie of Z rings in a liposome (movie S1 from [23]; see Fig. 1).

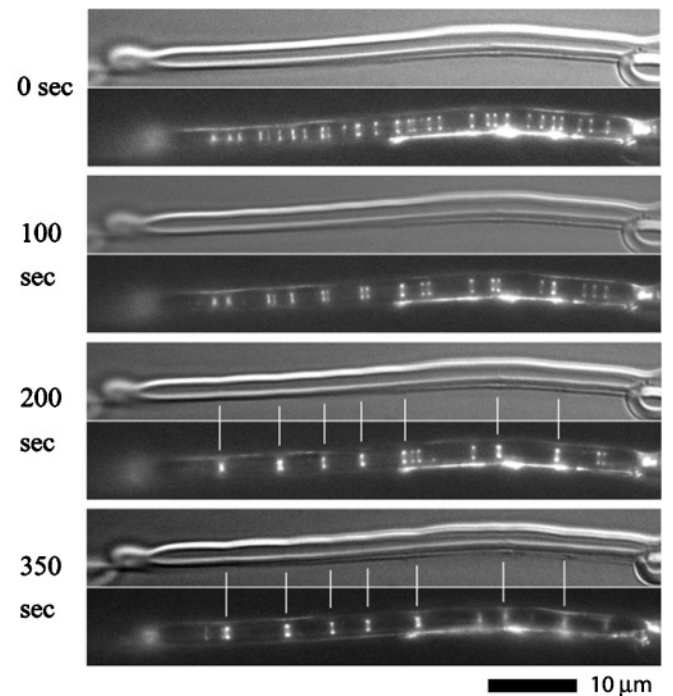


FIG. 1. Four time frames from movie S1 from [23]. Initially there are many dim rings and no obvious invaginations. After several minutes, the rings have coalesced and ring-aligned invaginations are apparent (marked by white hash marks). Taken with permission from [23]. Scale bar added as per [1].

We estimate the drag coefficient of a fully developed Z ring ($\sim 10\,000$ subunits) moving along the liposome to be $0.01\text{--}0.02\text{ pN s nm}^{-1}$ and the bending modulus of the liposome wall to be $500\text{--}700\text{ pN nm}$ (in movie S1 from [23]; this is likely to vary from liposome to liposome). If we assume that force is generated by the highly curved FtsZ conformation, we estimate the bending modulus of a FtsZ protofilament to be $310\text{--}390\text{ pN nm}^2$. However, if we assume that force is generated by the intermediate curvature conformation, we estimate the filament bending modulus to be no smaller than 1400 pN nm^2 .

II. DATA ANALYSIS

A. Ring tracking

To quantify the movement of the *in vitro* FtsZ rings, we analyzed movie S1 from Osawa *et al.* For each time frame, we calculated fluorescence intensity as a function of position along the liposome by generating a polygonal line scan along the length of the liposome and summing intensities transverse to the line scan. The line-scan time series was used to track the locations of rings through time.

We found the trajectories of all 29 rings in the region of interest (from the left edge to just left of the bubble near the middle of the frame), tracking by maximum intensity (see Fig. 2).

Several features are noteworthy. Initially, the rings were spaced $1.6 \pm 0.6\text{ }\mu\text{m}$ apart. Groups of two to five rings coalesced over the first 200 s with some random motion evident. Our analysis (discussed below) indicates that this coalescence was not driven by diffusion alone, consistent with the modeling assumptions of Shlomovitz and Gov [27]. After 325 s, the 29 rings had coalescence into nine rings. These rings were spaced roughly equally apart at $5.2 \pm 1.2\text{ }\mu\text{m}$. Except for a coherent leftward shift of the leftmost six rings after 350 s, the rings maintained these interring distances in an apparent steady state.

B. Rings constrict liposome

To determine the extent of the constrictions, we again carried out a frame-by-frame analysis of movie S1 from Osawa

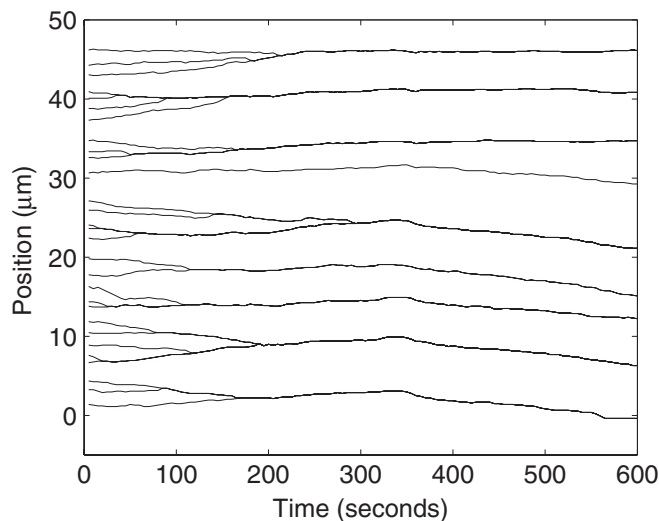


FIG. 2. Locations of rings along liposome in movie S1 from [23].

et al. Our algorithm extracted a portion of the differential interference contrast (DIC) image containing the region of interest and rotated the extracted image so that the liposome was horizontal. It then took neighboring pairs of single-pixel-width strips starting from the left edge to the right edge of the image (subsequently verified by going right to left) such that all strips crossed the bright band on the upper half of the liposome and carried out a cross-correlation on all such pairs. The maximum of the cross-correlation gave a relative vertical shift of membrane in the image from one strip to the next, without actually requiring that the exact location of the membrane be known. The strip-by-strip shifts were reassembled to construct the shape of the membrane. The shape was smoothed, and minima and maxima were identified. Successive min-to-max heights were calculated, and these values were used as an estimate of the extent of invagination as a function of time. The time course was fit to an exponential: $\epsilon(t) = \epsilon_0(1 - c_0 e^{-t/t_0})$. We found $\epsilon_0 \in [0.18, 0.20]$ with 95% confidence and an optimal value of 0.19, $c_0 \in [0.95, 1.2]$ with an optimal value of 1.1, and $t_0 \in [110, 167]$ with an optimal value of 138 s ($R^2 = 0.53$). Invaginations grew from 0 to 19% of the liposome radius with a time constant of 138 s. Note that we adopt a value of $c_0 = 1$ for subsequent calculations, which is within the reported confidence interval and corresponds to the simplest assumption that the rings do not generate constrictions initially ($c_0 = 1.1$ corresponds to “negative” constrictions).

To estimate the initial ring radii, we measured the distances between the ring-marking bright spots in the fluorescence images in the first frame of the movie and got an average of $R_0 = 0.55\text{ }\mu\text{m}$. Note that this figure is smaller than previously reported [27,30]; we used a conversion factor of 10.8 pixels per μm [1]. We also measured the full constriction time course in the same manner, but this approach was less reliable than the DIC cross-correlation technique due to changes in the focal plane throughout the movie. To the extent that the constriction measurement results from the fluorescence images were reliable, they provided qualitative agreement with the DIC cross-correlation technique.

C. Estimating the number of subunits in the rings

In order to estimate the number of subunits in the rings, some analysis of the fluorescence data was required. From the initial and final line scans, several features are evident. Initially, a diffuse background intensity was present and rings had relatively low peak intensities. By integrating the fluorescence intensity, truncating the profiles at the base of each ring’s peak, we estimated that 70% of the FtsZ was in the diffuse signal and the rest was incorporated into rings. For accurate temporal comparisons, we adjusted image intensities for photobleaching and made several minor changes in the focal plane. At 600 s, the diffuse background intensity was gone and peak ring intensities were significantly higher than could be explained by coalescence of the original rings. The decay of the background intensity (during the final 200 s) occurred with a time constant of roughly $\tau = 105\text{ s}$. We assume this represents incorporation of subunits from the lumen into the rings.

We estimated the volume for the section of liposome in movie S1 within the region of interest to be $44\text{ }\mu\text{m}^3$. The

number of rings in the initial and final images were 29 and 9 respectively. The bulk concentration was reported by Osawa *et al.* to be $4 \mu\text{M}$. Assuming equal concentrations inside and outside the liposome, this indicates a total of around 100 000 subunits in this section of liposome. Given the 70% initial background signal, each ring therefore initially consisted of roughly $S_i = 1000$ subunits, meaning that the rings were 1–2 protofilaments thick. After 600 s, the rings had grown to roughly $S_f = 12\,000$ subunits, roughly 13 protofilaments thick.

III. MODELING

A. Filament incorporation can proceed by diffusion

Treating the liposome as a one-dimensional strip, we modeled the motion of FtsZ protofilaments along the length of the tube by a diffusion process on a finite domain bounded at each end by a Z ring. We considered the Z rings to be perfect absorbers, interpreted as Dirichlet boundary conditions. Defining the concentration of protofilaments to be $u(x, t)$, this function satisfies the equation $u_t = Du_{xx}$, with $u(0, t) = u(L, t) = 0$, where $L = 5.2 \mu\text{m}$ is the interring spacing (at most). The slowest decaying mode of the solution is $u_1(x) = \sin(\pi x/L)$ with decay time constant $\tau = L^2/(\pi^2 D)$. Equating this to the measured time constant for interring depletion of fluorescence ($\tau = 105$ s), we estimate the diffusion coefficient to be roughly $D = 0.03 \mu\text{m}^2/\text{s}$. This means that a protofilament diffusion coefficient of no less than this quantity would be required in order for diffusion to explain the arrival of protofilaments at the Z rings. A typical membrane-bound protein in a vesicle has a diffusion coefficient in the range $D_1 = 3 - 6 \mu\text{m}^2/\text{s}$ [31]. Previous measurements of *in vitro* polymer found that protofilaments are an average of 30 subunits long [32], so a crude estimate for their diffusion coefficient (assuming drag on subunits is additive) would be $D = D_1/30 = 0.1\text{--}0.2 \mu\text{m}^2/\text{s}$. In Secs. III B 5 and III B 7, we develop and test a more rigorous model for the drag on protofilaments and on the full ring, which supports our assumption that drag is additive. We conclude that diffusion of membrane-bound polymerized subunits is sufficient to explain the rate of filament delivery to the Z rings and that membrane-mediated interfilament forces, as suggested by Shlomovitz and Gov [27], although possible, are not required for filament delivery. Of course, without membrane-mediated interfilament forces, lateral binding or some other mechanism is required for ring cohesion.

B. Estimating Z-ring and liposome mechanical constants

Our primary interest here is in estimating the bending modulus of a FtsZ filament. To do so, we propose a mechanical model for the interaction between a Z ring and the multilaminar liposome wall that allows us to predict the extent of membrane indentation as a function of the ratio of the bending modulus of a FtsZ-filament to that of the liposome wall. Thus, using our measurement of liposome constriction, we can estimate the ratio of moduli. This reduces the problem of estimating the FtsZ filament bending modulus to estimating the bending modulus of the liposome wall. For this latter challenge, we propose a dynamic model for ring movement which describes the time-dependent interaction of rings as mediated

by the liposome; the liposome mechanical model provides the interring forces.

1. Z-ring constriction force

We use the Z-ring mechanical model of Allard and Cytrynbaum [12] to calculate the energy stored in a Z ring of radius R_z and use that to find the constriction force:

$$F_z(R_z) = -\frac{dE_Z}{dR_z} = \frac{B_f \delta S}{R_z^3} (f_c \kappa R_z - 1), \quad (1)$$

where B_f is the filament bending modulus, δ is the size of a FtsZ monomer, S is the number of monomers in a Z ring, f_c is the fraction of the monomers that are in a curved conformation, and κ is the preferred curvature of that conformation. Filaments are either straight or curved, and we use either $\kappa = 0.01 \text{ nm}^{-1}$ or $\kappa = 0.08 \text{ nm}^{-1}$.

2. Membrane energy

For the membrane energy, we propose the following model, which is related to several recently proposed models for Z rings in tubular liposomes [27,30]. Because the liposome is approximately axially symmetric, the shape of the liposomes is well described by a function $R(s)$, which gives the liposome radius as a function of position s along the length. We define $r(s)$, the fractional extent of constriction: $r(s) = [1 - R(s)/R_0]/\epsilon$, where $\epsilon = 1 - R_z/R_0$ is the maximal invagination (at the location of the rings). Note that ϵ changes with time as the rings incorporate more subunits. This time-dependent function is precisely the $\epsilon(t)$ reported above. R_0 is the preferred radius of the cylindrical liposome in the absence of rings. The value of $r(s)$ varies between 0, corresponding to an undeformed cylindrical shape with radius R_0 , and 1, corresponding to the invaginated membrane being in contact with the Z ring. Mechanical equilibration is rapid so the only time dependence of the mechanical problem comes through the empirically determined progression of invagination, $\epsilon(t)$, and through the movement of rings, a model for which is described Sec. III B 6.

The Z rings are attached to the inner liposome surface by amphipathic helices on the FtsZ subunits. We treat this attachment mechanism as a continuum of springs with per-surface-area spring constant k_s . Because the attachment distance is nonzero, $r(s)$ is never quite equal to 1. This is illustrated in Fig. 3.

We include both membrane bending and spring extension in the membrane energy. As the liposomes in Osawa's experiments have a preference for a cylindrical form in the absence of Z rings, we also include an energy term to

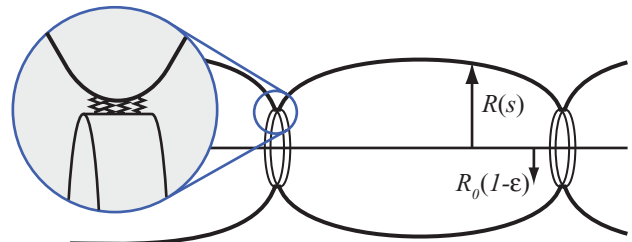


FIG. 3. (Color online) Illustration of the membrane energy model.

account for deviations from that preferred form. We omit membrane stretch because parts of the liposome can be seen to reshape themselves (e.g., the bubble in the middle of the frame in movie S1), indicating that the liposomes are leaky or that excess membrane is present. The leakiness of these

liposomes is described in subsequent work from the same laboratory [21]. The total energy, to leading order in ϵ , when the rings have radius R_z and are located at points x_i ($i = 1 \dots n$) and when the membrane has arbitrary shape given by $r(s)$, is

$$E_{\text{mem}}[r(s)] = \epsilon^2 \pi B_m \left(\int [r''(s)^2 + r(s)^2] ds + \Omega \sum_{i=1}^n \int_{x_i-w/2}^{x_i+w/2} [1 - r(s)]^2 ds \right), \quad (2)$$

where $\Omega = k_s R_0^4 / B_m$, B_m is the membrane bending modulus, and w is the width of each Z ring. Although the first integral expression can be derived using the formalism presented in Sec. 2.1 of the supplemental material of Lan *et al.* [13] for the shape of an *E. coli* cell wall by omitting dependence on the material coordinates, it is not obvious that the physics of such a description is appropriate here, and so we present this energy expression as a phenomenological model. The $r''(s)^2$ term accounts for longitudinal curvature. The circumferential curvature is negligible (higher order in ϵ) compared to the cylindrical restoring force $r(s)^2$ and so is omitted. The justification for the same modulus on both terms comes from data and Occam's razor—in short, if these moduli were not the same order of magnitude, the invaginations would be thin grooves or undetectably broad.

Finding the shape $r(s)$ that minimizes the energy requires that we solve the Euler-Lagrange equation

$$r'''' + r + \Omega \chi_w (r - 1) = 0, \quad (3)$$

where χ_w is the characteristic function of the collection of intervals on which rings are present, $\cup_{i=1}^n [x_i - w/2, x_i + w/2]$. At the edges of the rings, we impose matching conditions, enforcing that all derivatives up to third order are continuous, and we also require that r be bounded on the whole real line.

Solving this piecewise linear equation gives us the minimum energy profile $r_{\text{min}}(s)$, which we plug back in to get the energy when the membrane achieves its optimum:

$$E_{\text{mem}}^{eq}(R_z; x_1, \dots, x_n) = E_{\text{mem}}[r_{\text{min}}(s)] = \epsilon^2 \pi B_m \Gamma = \left(1 - \frac{R_z}{R_0}\right)^2 \pi B_m \Gamma(x_1, \dots, x_n), \quad (4)$$

where Γ is the integral expression in parentheses above and depends only on the relative positions of the rings x_i , their widths w , and the nondimensional spring constant Ω . Note that solving the Euler-Lagrange equation and calculating the minimum energy can be carried out analytically but involves solving a system of $8n + 4$ equations for the coefficients on each piece of $r(s)$ where n ranges from 29 down to 9. We used MATLAB (MathWorks, MA) and an “automatic differentiation” package [33] to set up and solve the matrix problem. The numerical results are not sensitive to Ω provided it is larger than 1000; fortunately, for Ω smaller than this, the spring extension ends up much larger than the size of an α helix, which means that such a parameter regime is unphysical. Sensitivity to w

is also weak; a 10-fold change in w leads to less than a 10% change in Γ . We used a value of $w = 0.03 \mu\text{m}$, which is a rough average based on our subunit estimates.

3. Force balance for a single ring

With only one ring present, taking the derivative of E_{mem}^{eq} with respect to R_z gives the force exerted by the membrane against the ring. The R_z dependence in the energy comes only through ϵ . The membrane and Z-ring forces must balance:

$$F_z(R_z) = \frac{B_f \delta S}{R_z^3} (f_c \kappa R_z - 1) = 2 \left(1 - \frac{R_z}{R_0}\right) \frac{B_m \pi \Gamma_1}{R_0} = F_{\text{mem}}^{eq}(R_z), \quad (5)$$

where $\Gamma_1 = 2.8$ is the appropriate Γ value for a single ring. This can be rewritten as

$$B_f = \phi B_m, \quad (6)$$

with

$$\phi = \frac{2\pi R_0^2 \Gamma_1 r_z^3 (1 - r_z)}{\delta S \psi r_z - 1}, \quad (7)$$

where $r_z = R_z / R_0$ and $\psi = f_c \kappa R_0$. By replacing parameters with their estimates discussed above, Eq. (5) becomes

$$\phi = 11 \text{ nm} / (0.81 \psi - 1), \quad (8)$$

where we have used $R_z = (1 - \epsilon)R_0$ with $\epsilon = 0.19$, $R_0 = 550 \text{ nm}$, $\delta = 4 \text{ nm}$, and $S = 12\,000$.

In order to determine ψ , we need to make some assumptions about filament curvature. If we assume that filaments are initially straight, then hydrolyze their GTP, and try to bend into the highly curved conformation ($\kappa = 0.08 \text{ nm}^{-1}$), with kinetics as discussed by Allard and Cytrynbaum [12] (giving us $f_c = 0.5$), then we find a value of $\psi = 22$ and so $\phi = 0.65 \text{ nm}$.

However, if we consider the possibility that the force is generated by filaments making the transition from the straight to intermediate conformation, the appropriate curvature is $\kappa = 0.01 \text{ nm}^{-1}$. Without data or a model for the fraction of filaments in the curved state, we leave f_c as a parameter that can range between 0 and 1 so that $0 < \psi < 5.5$, which gives us $\phi > 3 \text{ nm}$. We could provide an upper bound on ϕ if more were known about the kinetics of the conformation change.

4. Forces between multiple rings

For simplicity, in the multiring case, we assume that all rings have the same radius R_z . Note that the solution $r_{\text{min}}(s)$

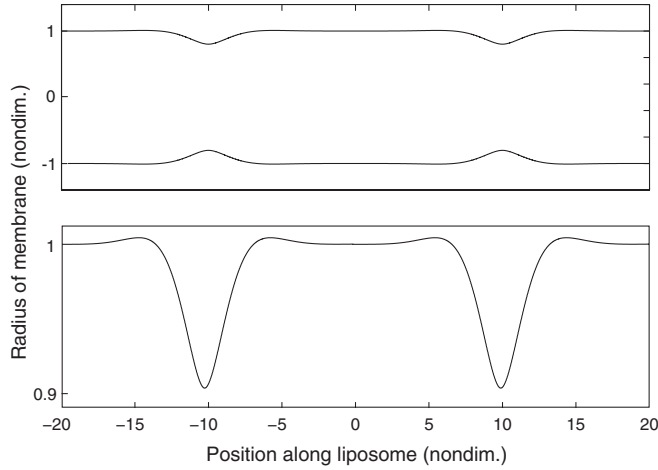


FIG. 4. The membrane shape that minimizes the energy when two rings are present. Top: shape of liposome with two rings. Bottom: close-up of upper membrane showing invaginations and oscillating “overshoot.”

consists, piecewise, of superpositions of functions of the form $\exp(\pm\alpha s)\cos(\alpha s)$ and $\exp(\pm\alpha s)\sin(\alpha s)$, where α is either $1/\sqrt{2}$, away from the rings, or $(1 + \Omega)^{1/4}/\sqrt{2}$, on the ring intervals. Thus, the membrane overshoots the preferred radius R_0 , oscillating and decaying with distance from the rings (see Fig. 4).

This oscillatory profile indicates that in the case of two rings, we expect to see a minimum in the total energy at a nondimensional separation distance of roughly $2\sqrt{2}\pi \approx 8.9$ (or dimensionally, $8.9R_0$), when the maxima to the left of the right ring and to the right of the left ring line up. In Fig. 5, one minimum can be seen at a zero-separation distance and a second can be seen at roughly 8.9 (circled for emphasis). Lesser minima at larger separation distances exist but are too small to be seen. For two rings, the first separated-ring minimum is asymmetric, with it being easier to drift apart than to drift together. For three rings, the middle ring sits in a robust well, as shown in Fig. 5, and the three are prevented from approaching each other. The outer two, however, can drift apart more easily, depending on the scale of the energy profile compared to $k_B T$.

The height of the energy barrier between the first two minima is roughly $\Delta\Gamma = 3$ in the direction of separation and $\Delta\Gamma = 0.3$ in the direction of coalescence. The barrier between the second and third (indiscernable) minimum is an order of magnitude smaller still. Given our eventual estimate of B_m , the barrier to coalescence has a height of $\Delta E = \epsilon^2\pi B_m \Delta\Gamma \approx 20$ pN nm, which, being roughly five times $k_B T$, is consistent with the lack of diffusion-driven coalescence events in the latter half of movie S1. The barrier between the second and third minima is comparable to $k_B T$ so drifting apart is feasible but depends on the diffusion coefficient and the observation time.

The nondimensional separation distance as measured in movie S1 was 9.5. Shlomovitz and Gov predicted a separation distance of 2π [27] and Horger *et al.* predicted a similar figure, ~ 7 [30].

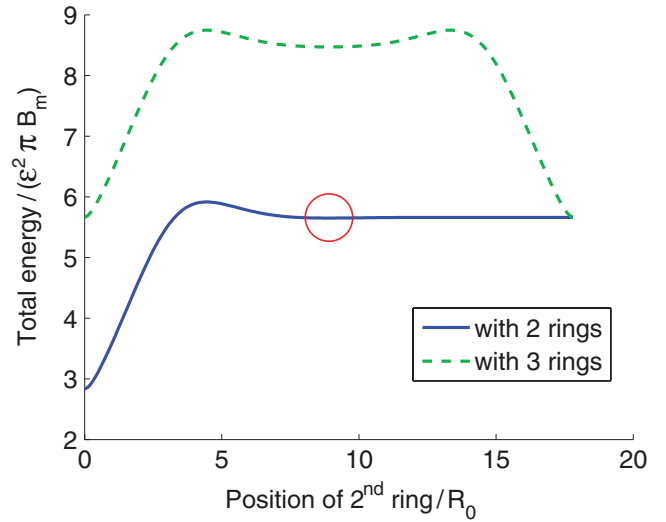


FIG. 5. (Color online) Nondimensional membrane energy (i.e., Γ) with two rings (solid, blue) and three rings (dashed, green) present. In the case of two rings, note the minimum at 8.9 (red circle). In the case of three rings, the outer two are placed roughly 17.8 nondimensional units apart.

5. Drag coefficient of a Z ring

To build a dynamic model for ring interaction and motion, we required a theoretical handle on the drag coefficient of an entire Z ring. The diffusion coefficient of single-membrane-bound proteins in liposomes has been measured to be in the range of $D = 3\text{--}6 \mu\text{m}^2/\text{s}$ [31]. With the Einstein relation, we can convert this into a drag coefficient of $\xi = 0.0007\text{--}0.0013$ pN s μm^{-1} . If the drag coefficient for a single protein were 0.001 pN s μm^{-1} and there was negligible interaction between neighbors in a ring, the drag coefficient on an early ring consisting of 1000 subunit would be 1 pN s μm^{-1} and the drag coefficient on a late ring of 13 000 subunits would be 13 pN s μm^{-1} .

To account for the possibility of non-negligible subunit interactions, we modeled the Z ring as a lattice of disks embedded in a rectangular two-dimensional (2D) domain, analogous to the approach taken by Saffman and Delbruck [29] for estimating the mobility of single proteins [which they refer to as case (i)], and numerically simulated the fluid flow in the intervening space. The top and bottom of the domain were identified (periodic boundary conditions) to create a cylindrical liposome. We solved the Stokes equation on this domain with no-slip boundary conditions at the edges of the embedded disks using a finite-element numerical scheme. We calculated a drag coefficient for the entire structure by finding the relationship between the imposed velocity field at the ends of the cylinder and the total resulting force on all subunits. The slope of such a velocity-force curve is the drag coefficient. We found that it scales approximately linearly in the number of protofilaments, except for minor deviations at fewer than four protofilaments. It was not particularly sensitive to the spacing between protofilaments (a factor of 1.5 variation between zero to infinite spacing). The greatest sensitivity was to the spacing between subunits in the circumferential direction, along a protofilament. The subunits bind to each

other in the hydrophilic domain (not explicitly modeled) but the drag coefficient properties are largely determined by the membrane fluid dynamics. As the disks represent the membrane-embedded domain, we fixed the distance between disk centers at 5 nm and varied the size of the disks. As the disks approached the size of the entire subunit, the drag coefficient grew due to the high pressure—fluid must squeeze through a narrow gap. The per-subunit drag coefficient ranged from $\sim 0.0012 \text{ pN s } \mu\text{m}^{-1}$ for disks with diameter 1 nm, consistent with the “negligible interaction” estimate, to $\sim 0.2 \text{ pN s } \mu\text{m}^{-1}$ for disks with diameter 4.4 nm, with blowup theoretically occurring at 5 nm since there is no space between neighboring subunits. The amphipathic helices that attached FtsZ to the liposomes in Osawa *et al.*'s study consisted of eight amino acids [34], which corresponds to a disk diameter of around 1.2 nm, leading to a predicted per-subunit drag coefficient of $\sim 0.0016 \text{ pN s } \mu\text{m}^{-1}$.

6. The N -body problem for Z rings

To calculate the trajectories of all Z rings in a liposome as they exert membrane-mediated forces on each other, we calculate the total energy in the membrane-ring system when the rings are located at positions x_i ($i = 1, \dots, n$) along the length of the liposome. We simplify the problem by assuming the variation in radius from ring to ring is negligible and prescribe a time-dependent evolution of the radius $R_z(t)$, and thus $\epsilon(t)$, caused by recruitment of FtsZ into the rings. This time-dependent behavior is extracted from the data, as described above, and fitted with the function $\epsilon(t) = \epsilon_0(1 - c_0 e^{-t/t_0})$. The drag coefficient of a ring moving along a liposome is also time dependent because the rings are constantly incorporating new subunits.

The lateral force on each ring is then calculated by taking the partial derivative of the membrane energy with respect to that ring's position:

$$F_i = -\frac{\partial E_{\text{mem}}^{\text{eq}}}{\partial x_i}(R_z; x_1, \dots, x_n) = \epsilon_0^2(1 - c_0 e^{-t/t_0})^2 \pi B_m \frac{\partial \Gamma}{\partial x_i}. \quad (9)$$

This force is then used in a Langevin equation for the position of each ring:

$$\frac{dx_i}{dt} = -\epsilon_0^2(1 - c_0 e^{-t/t_0})^2 \frac{\pi B_m}{\xi_{ps} S(t)} \frac{\partial \Gamma}{\partial x_i} + v(t), \quad (10)$$

where ξ_{ps} is the drag coefficient on a single FtsZ subunit and $v(t)$ is Gaussian white noise with autocorrelation $\langle v(t)v(\tau) \rangle = 2D(t)\delta(t - \tau)$, where $D(t)$ is the ring diffusion coefficient.

Under the assumption that diffusive motion is thermal (an assumption which we explore below), the diffusion coefficient is related to the drag by the Stokes-Einstein relation $D(t) = k_B T / \xi(t)$, where $\xi(t) = \xi_{ps} S(t)$ is the Z-ring drag coefficient. We set $S(t) = 1000 + 18t$, which linearly interpolates between the estimated initial 1000 subunits and final 12 000 subunits per ring. We used values of $c_0 = 1$ and $t_0 = 138 \text{ s}$ (from Sec. II B).

7. MCMC fitting of the ring drag coefficient and membrane bending modulus

We used a Markov Chain Monte Carlo (MCMC) parameter-estimation method [35] to find B_m and ξ_{ps} which best fit the observed time courses of lateral ring motion [36]. Combining the lateral ring position time series with the above model for lateral ring dynamics, we estimate $\xi_{ps} = 0.0012 \pm 0.0001 \text{ pN s } \mu\text{m}^{-1}$ and $B_m = 530 \pm 60 \text{ pN nm}$. The per-subunit drag coefficient agrees remarkably well with the above first-principles calculation of $0.0016 \text{ pN s } \mu\text{m}^{-1}$.

To explore the robustness of estimates with respect to model variations, we ran MCMC estimates on five variants of the N -body model given by Eq. (10). We variously assumed that subunit number is constant, $S(t) = S_0$, that ring radius is constant, $\epsilon(t) = \epsilon_0$, that diffusion is nonthermal (and hence not linked to drag, as described above) and either constant in time or inversely proportional to $S(t)$, and imposed the first-principles estimate of ξ_{ps} from Sec. III B 5 rather than fitting it. The resulting estimates of B_m , summarized in Table S1 of the supplemental material [37], are all within an order of magnitude of the above estimate, suggesting robustness of the estimate.

An example simulation with the estimated parameter values is shown in Fig. 6, juxtaposed against the experimental data from Fig. 2. Heuristically, the parameters determine two features of the simulated trajectories: The time required for coarsening is related to the ratio of the membrane bending modulus to the drag coefficient and the amplitude of the noise in the trajectories is related to the ratio of the thermal energy scale ($k_B T$) to the membrane bending modulus. A third feature, which is relatively insensitive to variation in the fitted parameters, is ring coalescence. The simulations correctly predict which of the 29 original rings end up in which of the nine final rings, for all except five initial rings. This behavior is largely determined by the width of the energy well shown in Fig. 5;

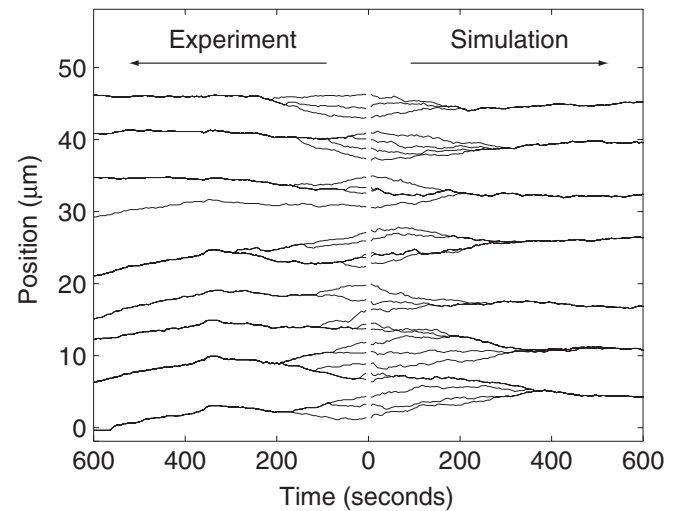


FIG. 6. A sample simulation of the trajectories of 29 Z rings using the MCMC-determined parameter values is shown on the right side of the axes. Initial conditions are taken from our measurements from the first time frame of Osawa *et al.*'s movie S1 [23]. The Z-ring trajectories shown in Fig. 2 are reproduced here, in reverse temporal orientation on the left for ease of comparison.

in principle, diffusion could also influence the process, but our results suggest that, at best, it does so only to a limited extent.

C. Filament bending modulus estimates

With an estimate for B_m in hand, we use Eq. (6) to relate the membrane bending modulus to the bending modulus for a single FtsZ protofilament. Adopting the highly curved conformation model, we predict $B_f = 350 \pm 40$ pN nm². If we adopt the intermediate-curvature model instead, we predict $B_f > 1400$ pN nm².

IV. DISCUSSION

The data analysis and modeling presented here provide a relatively indirect means of estimating parameters relevant to the *in vivo* context that have been otherwise difficult to determine. When we assume that force is generated by the posthydrolysis, highly curved conformation of FtsZ, our estimate of the FtsZ-filament bending modulus, 310–350 pN nm², falls at the lower end of the range of values that have been previously estimated and/or used in modeling studies. When we adopt the intermediate-curvature conformation as the force-generating state, we estimate that the bending modulus is no less than 1400 pN nm². Our estimate for the membrane bending modulus, which is independent of the FtsZ-conformation assumption, is 500–700 pN nm.

The former estimate of the FtsZ bending modulus (310–350 pN nm²) lends support to some previous estimates [17,18]. Nonetheless, it deviates from measurements of other cytoskeletal filaments, notably microtubules and actin, which have similar Young's moduli [38]. Gittes *et al.* [38] pointed out that microtubules and actin have a stiffness comparable to other filamentous proteins such as silk, keratin, wool, and collagen but are thousands of times stiffer than other rubberlike filamentous proteins (elastin, resilin, abductin). Thus, a universal Young's modulus for filamentous proteins should not be expected. However, it would be surprising for two structurally homologous filaments such as microtubules and FtsZ protofilaments to differ in their stiffnesses by more than an order of magnitude. A final caveat that must be considered is that a Young's modulus, whose definition depends on a continuum cross section, might be well defined for filamentous structures with cross-sectional areas consisting of many subunits, but for single-protein cross sections with only a small number of bonds, it may be ill defined or subject to greater sensitivity to the details of protein structure.

The latter estimate of the FtsZ bending modulus (>1400 pN nm²) is more consistent with the idea of a single cytoskeletal Young's moduli, but this lower bound is still on the small side as the tubulin-homology-based estimate is 10

times larger. The lack of an upper end to this range is due to the lack of an estimate of the fraction of filaments in the intermediate conformation (f_c).

As suggested by Lan *et al.* [13], if the filament bending modulus is as low as 1400 pN nm² (or lower), the maximum force a filament could produce is in the range of a few piconewton or smaller. In such a scenario, according to their earlier estimate of the force required for cell-wall invagination (8 pN) [39], the filament-curvature-mediated mechanism for force generation is too low to be feasible [12]. However, this is a highly theoretical conclusion, depending on the correctness and accuracy of several models. More direct experimental measurement of both the bending modulus and required invagination force are critical for resolving this force-generation mystery. A clearer understanding of the role played by the intermediate-curvature conformation is also essential.

Interpreting our estimate of the membrane bending modulus, we note that it is somewhere between the estimates of Shlomovitz *et al.* [27] (40–400 pN nm) and Horger *et al.* [30] (10 000 pN nm), closer to the former. Horger *et al.* arrived at their figure by assuming the multilaminar liposome wall consisted of roughly 125 individual lipid bilayers. Presumably, this was estimated from the thickness of the wall in Osawa *et al.*'s DIC images. Such images are not ideal for extracting accurate geometric details, which may explain the difference. Shlomovitz *et al.* did not provide a rationale for their number but it is consistent with a 1- to 5-layer wall. Our bending modulus estimate suggests, at least for the liposome in movie S1, about 6–12 layers in the liposome wall.

Our most verifiable and hence convincing estimate is that of the drag coefficient on the ring. The simplest approach, of using a measured diffusion coefficient and the Einstein relation, gave us a crude estimate for the per-subunit drag (0.001 pN s μm^{-1}) that was close to both the figure arrived at using the fluid model (0.0012 pN s μm^{-1}) and the MCMC method (0.0016 pN s μm^{-1}). Given that the MCMC drag estimate was consistent with the other approaches, it lends some credibility to the MCMC-derived estimate of the membrane bending modulus. Further supporting our estimate of the membrane bending modulus is the fact that, to within a factor of 2, the estimate was robust to several perturbations of the modeling assumptions, as described in the supplemental material [37].

ACKNOWLEDGMENTS

The authors thank H. Erickson and M. Osawa for useful feedback. This work was supported by the National Science and Engineering Research Council.

-
- [1] H. P. Erickson, D. E. Anderson, and M. Osawa, *Microbiol. Mol. Biol. Rev.* **74**, 504 (2010).
 [2] H. P. Erickson, D. W. Taylor, K. A. Taylor, and D. Bramhill, *Proc. Natl. Acad. Sci. USA* **93**, 519 (1996).
 [3] A. Mukherjee and J. Lutkenhaus, *J. Bacteriol.* **181**(3), 823 (1999).

- [4] L. Romberg, M. Simon, and H. P. Erickson, *J. Biol. Chem.* **276**, 11743 (2001).
 [5] J. Lowe and L. A. Amos, *EMBO J.* **18**, 2364 (1999).
 [6] J. M. Gonzalez *et al.*, *J. Biol. Chem.* **278**, 37664 (2003).
 [7] M. A. Oliva *et al.*, *J. Biol. Chem.* **278**, 33562 (2003).

- [8] G. Lan, A. Dajkovic, D. Wirtz, and S. X. Sun, *Biophys. J.* **95**, 4045 (2008).
- [9] H. P. Erickson, *Proc. Natl. Acad. Sci. USA* **106**, 9238 (2009).
- [10] B. Ghosh and A. Sain, *Phys. Rev. Lett.* **101**, 178101 (2008).
- [11] I. Horger *et al.*, *Phys. Rev. E* **77**, 011902 (2008).
- [12] J. F. Allard and E. N. Cytrynbaum, *Proc. Natl. Acad. Sci. USA* **106**, 145 (2009).
- [13] G. Lan *et al.*, *Proc. Natl. Acad. Sci. USA* **106**, 121 (2009).
- [14] D. A. Drew *et al.*, *Bull. Math. Biol.* **71**, 980 (2009).
- [15] Z. Li, M. J. Trimble, Y. V. Brun, and G. J. Jensen, *EMBO J.* **26**, 4694 (2007).
- [16] G. Fu *et al.*, *PLoS ONE* **5**, e12682 (2010).
- [17] S. Huecas *et al.*, *Biophys. J.* **94**, 1796 (2008).
- [18] A. Dajkovic *et al.*, *Curr. Biol.* **18**, 235 (2008).
- [19] Y. Chen, K. Bjornson, S. D. Redick, and H. P. Erickson, *Biophys. J.* **88**, 505 (2005).
- [20] J. Mingorance *et al.*, *J. Biol. Chem.* **280**, 20909 (2005).
- [21] M. Osawa, D. E. Anderson, and H. P. Erickson, *EMBO J.* **28**, 3476 (2009).
- [22] B. Mickey and J. Howard, *J. Cell Biol.* **130**, 909 (1995).
- [23] M. Osawa, D. E. Anderson, and H. P. Erickson, *Science* **320**, 792 (2008).
- [24] M. Osawa and H. P. Erickson, *Mol. Microbiol.* **81**, 571 (2011).
- [25] C. Lu, M. Reedy, and H. P. Erickson, *J. Bacteriol.* **182**, 164 (2000).
- [26] A. Mukherjee, C. Saez, and J. Lutkenhaus, *J. Bacteriol.* **183**, 7190 (2001).
- [27] R. Shlomovitz and N. S. Gov, *Phys. Biol.* **6**, 046017 (2009).
- [28] I. Horger *et al.*, *Biophys. J.* **94**, L81 (2008).
- [29] P. G. Saffman and M. Delbruck, *Proc. Natl. Acad. Sci. USA* **72**, 3111 (1975).
- [30] I. Horger, F. Campelo, A. Hernandez-Machado, and P. Tarazona, *Phys. Rev. E* **81**, 031922 (2010).
- [31] S. Ramadurai *et al.*, *J. Am. Chem. Soc.* **131**, 12650 (2009).
- [32] Y. Chen and H. P. Erickson, *J. Biol. Chem.* **280**, 22549 (2005).
- [33] R. D. Neidinger, *SIAM Rev.* **52**, 545 (2010).
- [34] T. H. Szeto, S. L. Rowland, C. L. Habrukowich, and G. F. King, *J. Biol. Chem.* **278**, 40050 (2003).
- [35] W. H. Press, S. A. Teukolsky, W. T. Vetterling, and B. P. Flannery, in *Numerical Recipes*, 3rd ed. (Cambridge University Press, Cambridge, 2007), pp. xxii, 1235.
- [36] See Supplemental Material at <http://link.aps.org/supplemental/10.1103/PhysRevE.85.011902> for details of the MCMC methods.
- [37] See Supplemental Material at <http://link.aps.org/supplemental/10.1103/PhysRevE.85.011902> for a table showing the MCMC results for six variants of the basic model.
- [38] F. Gittes, B. Mickey, J. Nettleton, and J. Howard, *J. Cell Biol.* **120**, 923 (1993).
- [39] G. Lan, C. W. Wolgemuth, and S. X. Sun, *Proc. Natl. Acad. Sci. USA* **104**, 16110 (2007).